

6 AVIATION FA 8.5

FORECAST SKILL OF A HIGH-RESOLUTION REAL-TIME MESOSCALE MODEL
DESIGNED FOR WEATHER SUPPORT OF OPERATIONS
AT KENNEDY SPACE CENTER AND CAPE CANAVERAL AIR STATION

John Manobianco* and Gregory E. Taylor
ENSCO, Inc. / Applied Meteorology Unit / NASA
Kennedy Space Center, FL

and

John W. Zack
MESO, Inc.
Troy, NY

1. INTRODUCTION

Weather support of ground and spaceflight operations at NASA's Kennedy Space Center (KSC) and the Air Force's Eastern Range at Cape Canaveral Air Station (CCAS) requires short range (< 24 h), detailed forecasts of winds, clouds, ceilings, fog and severe weather such as heavy rain and lightning. The implementation of a local, mesoscale modeling system at KSC/CCAS is designed to provide accurate forecasts of specific thunderstorm-related phenomena such as precipitation and high winds thereby reducing downtime due to false weather advisories and alerts, hazardous weather events occurring without warning, and unnecessarily restrictive weather-based flight rules for manned and unmanned missions.

In order to meet the forecasting needs at KSC/CCAS, NASA funded Mesoscale Environmental Simulations and Operations (MESO), Inc. to develop a version of the Mesoscale Atmospheric Simulation System (MASS). The model has been modified specifically for short-range forecasting in the vicinity of KSC/CCAS. To accomplish this, the model domain has been limited to increase the number of horizontal grid points (and therefore grid resolution) and the model's treatment of precipitation, radiation, and surface hydrology physics has been enhanced to predict convection forced by local variations in surface heat, moisture fluxes, and cloud shading.

The objective of this paper is to (1) provide an overview of MASS including the real-time initialization and configuration for running the data pre-processor and model, and (2) to summarize the preliminary evaluation of the model's forecasts of temperature, moisture, and wind at selected rawinsonde station locations during February 1994 and July 1994.

2. MASS MODEL OVERVIEW

MASS is a hydrostatic, three-dimensional modeling system which includes schemes to represent planetary boundary layer processes, surface energy and moisture budgets, free atmospheric long and short wave radiation,

cloud microphysics, and sub-grid scale moist convection. The first documented version (2.0) was described by Kaplan et al. (1982). The latest version (5.5) has been improved by adding data assimilation capabilities based upon Newtonian relaxation, enhancing the representation of physical processes in the surface energy and moisture budgets, and optimizing the computational efficiency of the model software on workstation platforms. A detailed description of version 5.5 and enhancements to MASS developed for specific application to forecasting at KSC/CCAS are provided elsewhere (MESO, 1993; Zack et al. 1993).

A 45 km horizontal resolution version of the model is run over the southeastern United States to provide lateral boundary conditions for a one-way nested 11 km grid which is executed over a domain that covers the entire Florida peninsula, eastern Gulf of Mexico and western Atlantic Ocean. The vertical spacing of the model's 20 sigma layers used for both coarse and fine grid runs varies from ~20 m at the lower boundary (i.e. the surface) to ~2 km at the upper boundary (i.e. 100 mb).

2.1 Real-time MASS Initialization

There are a number of in-situ and remotely-sensed data sources that are presently used to initialize the MASS model. The gridded data from the National Meteorological Center's (NMC) Nested Grid Model at 2.5° latitude by 1.25° longitude resolution provides first-guess fields for the analysis of all available data and boundary condition values throughout the forecast. The MASS model incorporates standard synoptic data (e.g. rawinsonde, surface), local data (e.g. KSC/CCAS mesonet observations), and data derived from sensing systems that do not directly measure model variables (e.g. latent heating rates from radar-estimated precipitation rates).

2.2 Real-time MASS Configuration

The MASS pre-processor and model have been run twice daily on a four-processor Titan 3000 workstation since December 1993. The real-time model runs and observations are being archived until October 1994 to generate the data base needed for model evaluation.

*Corresponding author address: Dr. John Manobianco, ENSCO, Inc., 445 Pineda Court, Melbourne, FL 32940.

The daily model forecast and data assimilation schedule consists of two 24-h coarse grid and two 12-h fine grid runs per day. The 24-h coarse grid run designated C00 is initialized with 0000 UTC data and assimilates hourly surface and manually digitized radar (MDR) data from 0000-0400 UTC. The 12-h fine grid run designated F12 is initialized with 1200 UTC data and assimilates 1300 UTC surface and MDR data. The 12-h forecast from C00 (valid at 1200 UTC) provides the first guess fields for the objective analysis of 1200 UTC data used for F12 initialization. Additionally, the 12-24 h forecast fields from C00 are used to specify boundary conditions for the F12 run. The cycle is repeated using 1200 UTC data to initialize the 24-h coarse grid run designated C12 and 0000 UTC data to initialize the 12-h fine grid run designated F00.

3. MASS EVALUATION

The results presented in this section focus on the objective evaluation of model forecasts at selected rawinsonde station locations. The skill of coarse and fine grid temperature, moisture, and wind forecasts at rawinsonde stations is assessed by interpolating the model data to the observation locations and then computing the bias and root mean square error (RMSE). Station comparisons provide a stringent test of model capabilities since statistics computed for many grid points do not assess model forecast skill at individual locations. However, station observations sample many scales of atmospheric phenomena some of which can not be resolved by the model. As a result, point verification should benefit higher resolution models which resolve finer scales of motion but it does tend to give a more pessimistic view of model performance than gridded verification. Nevertheless, model skill scores for stations are of more interest to end users of model guidance since, ultimately, forecasters want to know how accurately the model can predict the weather at specific locations.

3.1 Methodology

The analyses and forecast fields from all available 0000 UTC and 1200 UTC coarse grid forecasts during February 1994 and July 1994 have been bilinearly interpolated to the rawinsonde station locations given in Table 1. This list includes all available rawinsonde sites within the fine grid domain and selected sites within the coarse grid domain. The months of February and July have been chosen for the initial comparison of model performance during winter and summer.

TABLE 1 List of rawinsonde stations	
Station number	Location
72407	Atlantic City, NJ
72340	Little Rock, AR
72327	Nashville, TN
72213	Waycross, GA
72235	Jackson, MS
72210	Tampa Bay, FL
72203	West Palm Beach, FL
72201	Key West, FL
74794	Cape Canaveral, FL

The two statistical measures used here to quantify model forecast skill are the bias and RMSE. The bias is computed as:

$$\text{bias}(p, t) = \frac{1}{N} \sum_{n=1}^N (\Phi_f - \Phi_o) \quad (1),$$

and the RMSE is computed as:

$$\text{RMSE}(p, t) = \left[\frac{1}{N} \sum_{n=1}^N (\Phi_f - \Phi_o)^2 \right]^{1/2} \quad (2).$$

In Equations (1) and (2), Φ denotes temperature ($^{\circ}\text{C}$), dew point temperature ($^{\circ}\text{C}$), wind speed (ms^{-1}) or wind direction ($^{\circ}$) and the subscripts f and o denote forecast and observed quantities, respectively. In cases where the magnitude of the wind direction deviation (i.e. forecast minus observed) exceeds 180° , the deviation is recomputed by first subtracting 360° from the larger of the forecast or observed wind direction.

The subscript n in Equations (1) and (2) refers to an individual model run and N is the total number of coarse grid runs initialized at 0000 UTC (C00) and 1200 UTC (C12). The bias and RMSE for each variable are a function of pressure and time. These quantities are computed at 50 mb intervals from 1000 mb to 150 mb for the analysis times (0 h), and the forecasts times (12 h, 24 h) at 12-h intervals corresponding to the standard rawinsonde observation times. Errors which are greater than two standard deviations from the mean forecast minus observed differences are removed. This objective procedure is very useful in flagging bad data points.

3.2 Temperature Bias and RMSE

The temperature (T) bias ($^{\circ}\text{C}$) for February and July are shown in Figures 1a and 1b, respectively. The statistics have been averaged for all stations in Table 1 and include both C00 and C12 forecasts for each month. The number of deviations [N in Equations (1) and (2)] used to compute the bias and RMSE at any given level depends on the availability of both observations and model runs and is usually greater than 350 with a maximum 504 in February and 558 in July (i.e. number of days in the month \times two coarse grid cycles per day \times 9 stations).

The initial analyses show a negative (cool) bias for T in February on the order of -0.5°C between 950 mb and 300 mb (Fig. 1a). In July, the 0-h T bias at these same levels is very close to 0°C . The 0-h negative T bias increases to more than -1.0°C at 1000 mb in February, whereas in July, it actually becomes positive on the order of 0.5°C (Fig. 1b). Above 300 mb, the model shows a maximum positive (warm) bias for T of almost 1.0°C in February and 1.5°C in July. DiMego et al. (1992) also report a warm bias for T of 0.9°C at 250 mb for the 0-h forecasts from the Regional Analysis and Forecast System (RAFS) which is used to initialize the NGM. (Note that the RAFS was verified against 66 eastern North American rawinsonde observations for the period 24 March to 20 April 1991.) The bias in the MASS upper tropospheric T analyses for February and July is probably related to having insufficient vertical model resolution to resolve the temperature minima that are observed at the tropopause.

The 12-h coarse grid forecasts exhibit negative T biases except above 300 mb in both February and July. The negative T bias does not become substantially more negative by 24-h, although it does reverse sign becoming positive in the lower levels below 900 mb in February and below 800 mb in July. Above 300 mb, the 0-h warm bias for T actually increases slightly in the 12-h forecasts with very small changes thereafter in the 24-h forecasts during February and July (Figs. 1a and 1b).

The RMSE ($^{\circ}\text{C}$) for T at 0, 12, and 24 h during February and July are shown in Figures. 2a and 2b. The RMSE for T at 0 h for both months are less than 1.0°C between 950 mb and 300 mb and are on the order of the rawinsonde measurement errors for temperature. The MASS preprocessor uses a Barnes objective analysis procedure to blend first guess fields and observations into a consistent three-dimensional initialization data set. In general, the objective analysis scheme does not provide an exact fit to the data.

In February and July, the RMSE for T increase by a factor of 2 to 3 between the 0-h analyses and 12-h forecasts (Figs. 2a and 2b). There is a slight increase in RMSE for T at most pressure levels between the 12-h and 24-h forecasts in February, whereas in July, the only notable increase occurs below 900 mb. One explanation is that errors in forecasting the synoptic waves during February may lead to the increase in RMSE for T from the 12-h to 24-h coarse grid forecasts. Since there is less movement of weaker features during the summer (i.e. July), the error growth may be smaller in absolute terms than during the winter.

3.3 Dew Point Temperature Bias and RMSE

The dew point temperature (T_d) bias ($^{\circ}\text{C}$) for February and July are shown in Figures 1c and 1d, respectively. The analyses show a T_d bias of not more than 1°C below 500 mb during either month. The most notable feature in the analyses appears above 500 mb where the T_d bias is negative (i.e. too dry) in both February and July (Figs. 1c and 1d). The model develops a moist bias on the order of 3°C by 12 h in the February forecasts below 500 mb. By 24 h, a moist bias in these same runs exists at all levels below 300 mb and is as large as 4°C near 1000 mb and from 700 mb to 500 mb.

During July, the magnitude of the moist bias is smaller than during February especially in the middle troposphere between 800 mb and 300 mb in either the 12-h or 24-h forecasts. Note that the model also tends to moisten the upper troposphere during the July forecasts producing the largest positive bias of nearly 2°C at 24 h. Assuming no error in T, a 2°C T_d error at 300 mb yields a relative humidity error of $\sim 15\%$. Wilson (1993) also found a moist bias of nearly 10% in 300 mb RH averaged over seven 12-h forecasts during February 1989 using the Pennsylvania State University (PSU) / National Center for Atmospheric Research (NCAR) mesoscale model, version 4 (i.e. MM4).

The RMSE ($^{\circ}\text{C}$) for T_d during February and July from the analyses and forecasts are shown in Figures 2c and 2d, respectively. The 0-h RMSE for T_d increase with height (i.e. decreasing pressure) during both months. Except in the upper troposphere above 300 mb, the RMSE for T_d are larger in the 12-h forecasts than in the 0-h analyses for

both months. However, the 24-h RMSE for T_d in July are very similar to those at 12 h, whereas in February, they continue to increase reaching a maximum of greater than 7°C at 500 mb (Figs. 2c and 2d). In July, the maximum RMSE for T_d of greater than 6.5°C are found at 400 mb in the 12-h forecasts. The fact that the RMSE for T_d increases more rapidly in February than in July from 12-24 h is likely a result of the more dynamically active weather regimes which prevail during winter.

At present, there are no first guess NGM moisture fields provided above 300 mb. Therefore, the MASS preprocessor uses the last level of moisture information (in this case 300 mb) to derive first guess fields above that level by extrapolating relative humidity. Additionally, rawinsonde relative humidity measurements are considered unreliable at temperatures below -40°C . Furthermore, rawinsondes sample the atmosphere at specific points and are highly sensitive to whether the balloon passes through cloudy or clear areas. For these reasons, care must be exercised in interpreting the results that focus on the accuracy of the moisture analyses and forecasts especially in the upper troposphere above 400 mb.

3.4 Wind Speed Bias and RMSE

The wind speed bias (ms^{-1}) for February and July are plotted as a function of pressure in Figures 1e and 1f, respectively. In general the analyses and forecasts exhibit a negative (slow) bias except above 400 mb in July for the 12-h and 24-h forecasts. The slow bias in the analyses are less than 1.0 ms^{-1} between 900 mb and 300 mb. During February, the slow bias increases most rapidly between the 12-h and 24-h forecasts reaching nearly 3.0 ms^{-1} at the level of maximum wind speed in the upper troposphere (around 300 mb). In comparison, DiMego et al. (1992) found that the 12-h NGM forecasts exhibit a 6.2 ms^{-1} vector wind bias at 250 mb when verified against eastern North American rawinsondes during March and April 1991.

The 12-h forecasts from July display a negative bias of greater than -1.0 ms^{-1} between 800 mb and 500 mb which is much larger than the negative bias from the 24-h July forecasts at these same levels (Fig. 2f). Also, the largest positive bias of more than 1.0 ms^{-1} occurs in the 12-h July forecasts at 250 mb. At 1000 mb, the negative bias present in the 0-h February and July analyses changes sign in the 12-h forecasts and remains positive in the 24-h forecasts indicating that the low-level model wind speeds are too strong (Figs. 1e and 1f).

The RMSE (ms^{-1}) for wind speed in the February and July analyses is less than 2 ms^{-1} below 300 mb (Figs. 2e and 2f). During both months, the error growth is largest during the first 12 h of the forecasts. The RMSE for wind speed continue to increase from the 12-h to 24-h forecasts in February but not in July. The maximum RMSE for wind speeds occurs at the level where wind speeds are the largest in the upper troposphere. The maximum RMSE for wind speed is on the order of 6 ms^{-1} at 300 mb during February and is nearly 2 ms^{-1} greater than the maximum RMSE wind speed error at 250 mb in July. This result is consistent with the fact that on average, the wind speeds are larger and the tropopause and level of maximum wind speed are found at lower altitudes in winter than in summer.

3.5 Wind Direction Bias and RMSE

The wind direction bias ($^{\circ}$) is plotted in Figures 1g and 1h. During February, the bias from the 0-h analysis is nearly 0.0° above 950 mb. In July, the analyses show a small but consistent negative bias of not more than -2.3° at most levels. The 12-h forecasts from February exhibit a positive bias at virtually all pressure levels indicating a clockwise shift of forecast wind direction relative to the observed wind direction. The same statement applies to the 12-h July forecasts although the positive bias from 700 mb to 900 mb is somewhat larger than in February reaching a maximum of greater than 5° at 750 mb.

The positive bias present at 1000 mb in the 0-h analyses from February and July reaches almost 10° in the 12-h forecasts. The model develops a pronounced negative (counter-clockwise) bias on the order of -5° in the lower troposphere between 900 and 700 mb during the 24-h forecasts from February (Fig. 1g). A similar negative wind direction bias appears in the 24-h July forecasts at all levels above 850 mb.

A positive (clockwise) bias in the low-level wind direction during both months may be caused by underestimating the frictional forces in the planetary boundary layer. As a result, the forecast winds would tend to be more geostrophic since friction tends to rotate the winds counterclockwise relative to the isobars. If the low-level frictional stress is too weak, the winds would be too strong. This argument is consistent with a positive speed bias which does exist although only below 950 mb in the 12-h and 24-h forecasts (Figs. 1e and 1f).

The RMSE ($^{\circ}$) for wind direction during February and July are shown in Figures 2g and 2h, respectively. The RMSE for wind direction are largest at 1000 mb on the order of 20° in the analyses and decrease with height up to 300 mb. The same trend appears in the 12-h and 24-h forecasts during February with the maximum RMSE for wind direction of greater than 30° at 1000 mb for the 24-h forecasts. The amplitude of RMSE above 950 mb is larger in the July rather than February analyses. Compared with the 12-h February forecasts, the RMSE for wind direction increase more dramatically during the 12-h July forecasts. This result may be related due to the fact that the winds are in general weaker and more variable during the summer.

4. SUMMARY

The results presented in Section 3 highlight the preliminary evaluation of MASS model forecasts at selected rawinsonde sites for February 1994 and July 1994. The complete evaluation will consider error statistics for all model runs from January 1994 through October 1994. The assessment of model forecast skill will use an objective and subjective evaluation strategy.

The objective verification of MASS will include gridded comparisons of predicted and observed variables on the coarse grid, and station verification of temperature, moisture, and wind using surface data from synoptic sites, buoys, and KSC/CCAS mesonet towers. The accuracy of MASS model precipitation forecasts will be determined using high resolution rain gauge observations from the Florida water management districts. Finally, the subjective or phenomenological verification of the model will use a case study approach to document the success and failure of

the forecasts during specific weather regimes. The evaluation of MASS is scheduled for completion by the end of December 1994.

The goal of the evaluation is to determine how accurately MASS can predict the weather that impacts ground and aerospace operations at KSC/CCAS. At this point, it would be premature to assess the forecast skill of MASS based only upon the error statistics presented here. The possible explanations offered to account for the bias and RMSE shown in Figures 1 and 2 are very speculative. Additional diagnostics and more careful analyses of the results (such as stratification based upon initialization times, weather regimes, etc.) are needed to fully understand and explain these errors.

5. ACKNOWLEDGMENTS

The authors gratefully acknowledge AMU staff members Ann Yersavich and Devin Dean for assistance in data reduction and figure preparation.

6. REFERENCES

- DiMego, G.J., K.E. Mitchell, R.A. Petersen, J.E. Hoke, J.P. Gerrity, J.J. Tuccillo, R.L. Wobus, and H-M. H. Juang, 1992: Changes to NMC's Regional Analysis and Forecast System. *Wea. Forecasting*, **7**, 185-198.
- Kaplan, M. L., J. W. Zack, V. C. Wong, and J. J. Tuccillo, 1982: Initial results from a mesoscale atmospheric simulation system and comparisons with the AVE-SESAME I data set. *Mon. Wea. Rev.*, **110**, 1564-1590.
- MESO, 1993: *MASS Version 5.5 Reference Manual*, 118 pp. [Available from MESO, Inc., 185 Jordan Road, Troy, NY 12180].
- Wilson, K.B. 1993: Verification of cloud prediction from the PSU/NCAR mesoscale model. M.S. Thesis, The Pennsylvania State University, 116 pp.
- Zack, J.W., K.T. Waight, S.H. Young, M. Ferguson, M.D. Bousquet, and P.E. Price, 1993: *Development of a mesoscale statistical thunderstorm prediction system*. 203 pp. Final report to NASA under Contract No. NAS10-11670. [Available from MESO, Inc. 185 Jordan Road, Troy, NY 12180].

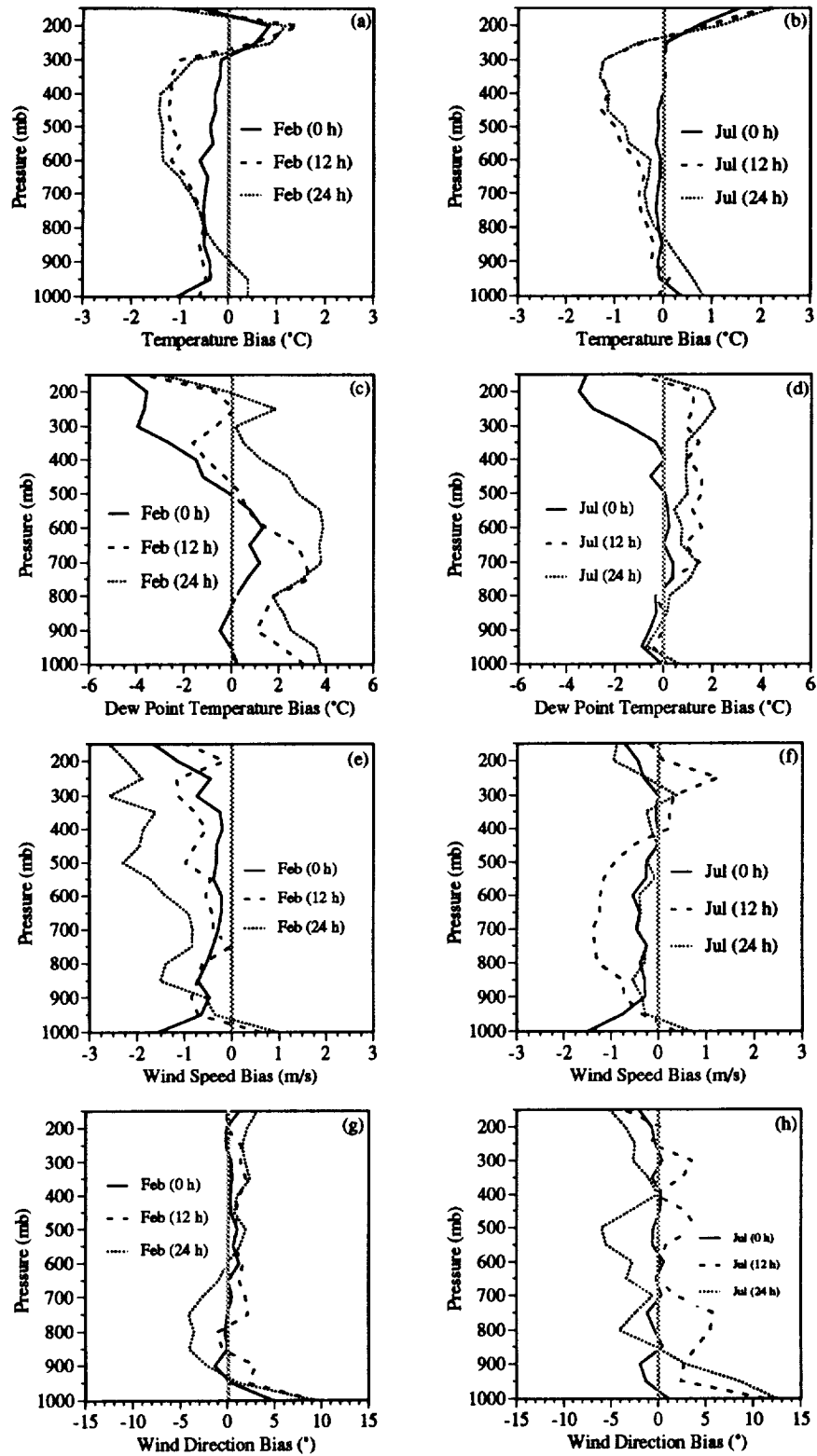


Figure 1. Average bias for temperature ($^{\circ}\text{C}$), dew point temperature ($^{\circ}\text{C}$), wind speed (ms^{-1}), and wind direction ($^{\circ}$) plotted as a function of pressure for February 1994 in panels (a), (c), (e), and (g), respectively, and for July 1994 in panels (b), (d), (f), and (h), respectively.

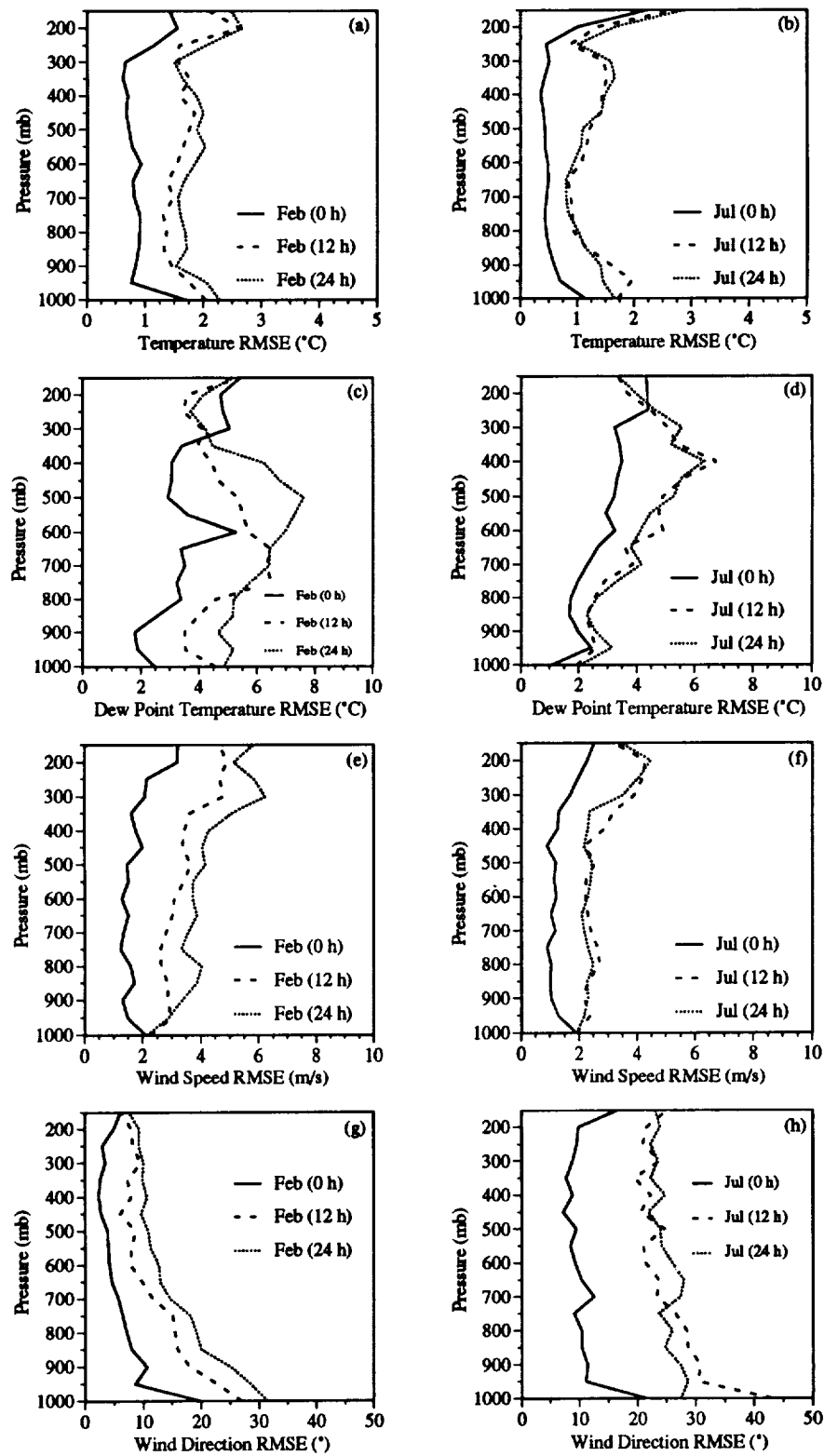


Figure 2. Average root mean square error for temperature ($^{\circ}\text{C}$), dew point temperature ($^{\circ}\text{C}$), wind speed (ms^{-1}), and wind direction ($^{\circ}$) plotted as a function of pressure for February 1994 in panels (a), (c), (e), and (g), respectively, and for July 1994 in panels (b), (d), (f), and (h), respectively.